Contents lists available at http://www.jmsse.org/

Journal of Materials Science & Surface Engineering

Establishing an empirical relationship to predict porosity and hardness of Titanium Oxide (TiO_2) coating deposited by High Velocity Oxy Fuel (HVOF) spraying

R. Sathiyamoorthy*, K. Shanmugam and V. Balasubramanian

Department of Manufacturing Engineering, Annamalai University, Annamalainagar – 608 002, Tamil Nadu, INDIA.

Article history

Received: 31-Dec-2014
Revised: 19-Jan-2015
Available online: 27th March, 2015

Keywords:
HVOF Spray,
Titanium oxide (TiO_2),
porosity,
hardness,
response surface methodology (RSM)

Abstract

Thermal sprayed Titanium dioxide (TiO_2) coating could be considered as candidate for the applications in the field of wear resistance, corrosion resistance and photo catalysis. High Velocity oxy Fuel (HVOF) spraying is a flexible and efficient method to deposit TiO_2 coating but the combination of the characteristics of the HVOF process with TiO_2 limits the usefulness of the coating. The HVOF parameters such as Oxygen flow rate, Fuel flow rate, powder feed rate and spray distance plays major role to control the coating properties such as porosity and hardness. In present study, an attempt has been made to develop empirical relationship to predict the porosity and hardness of the TiO_2 coating using response surface methodology (RSM). A central composite rotatable design with four factors and five levels was chosen to minimize the number of experimental conditions. The significant level of both the main effects and the interaction are observed by analysis of variance (ANOVA) approach, student's t-test, coefficient of determination was used to define the desired output variables through developing mathematical models to specify the relationship between the output responses and input variables. The porosity and hardness of the TiO_2 coating obtained within the range is highly influenced by fuel flow rate and spray distance. Further, a linear regression relationship was also established between porosity and hardness of the TiO_2 coating.

Introduction

Titanium dioxide (TiO_2) or Titania is a very important industrial material attracts much research attention owning to their promising application to photocatalytical, electrical, optical and tribological coatings [1-3]. The Titania coating engineered through thermal spray technique has excellent mechanical properties which potentially resist the wear by abrasion, erosion, and sliding [4-5]. Thermal sprayed Titania provide superior performance, life, and reliability to high pressure acid leach hydrometallurgical processing equipments, which employs autoclaves, valves and piping equipment in a severe high temperature acidic slurry environment [6-7]. It is well known that the Titania and other ceramics Al_2O_3, ZrO_2, Cr_2O_3 are processed by Atmospheric Plasma spraying due to high temperature of plasma jet which is necessary to melt the ceramics fully or partially to make coating. However, TiO_2 is ceramic material that has a relatively low melting point (1855° C) and it can be thermally sprayed via High Velocity Oxy Fuel (HVOF) process which is a technique that exhibits relatively low jet temperature (<3000°C) but high velocities. HVOF is a versatile method which can be used to deposit dense, adherent and homogeneous coatings with low porosity which is highly difficult to get dense coating through APS system [8-10].

The coating properties such as porosity, Young's modulus, phase uniformity and hardness determine to a large extent the performance in various applications. During HVOF spraying, the pores and microcracks can be generated from different sources, such as gas entrapment between impinging droplet and the rough surface, inadequate compaction of molten particles, splashing of droplets and micropores that can be result from crystallization of molten particles [11]. Porosity facilitates the crack initiation and propagation through splat boundary leading to exfoliation and delamination of ceramic coating. In case of dense coating, the hardness is high which resist the plastic deformation.

Since the coating properties are concerned about physical and chemical conditions such as pressure, temperature, velocity of flame which is strongly governed by numerous HVOF process parameters. Among those parameters Oxygen flow rate, Fuel flow rate, spray distance and powder particle size considered as primary influencing parameters. In conventional method, effect of some parameters on a process is performed by varying one parameter at a time. It is highly difficult to study one-factor at a time interaction approach which requires prohibitively large numbers of trials. Statistical designs of experiments have been shown to provide efficient approaches to systematically investigate the process parameters of thermal spray [12]. Researchers across the globe tried to model thermal spraying process using statistical regression techniques. Gill et al. Carried out the 3^3 factorial design experiments to establish the variables on the coating quality in relation to the corrosion behavior of HVOF sprayed Ni-based self fluxing alloys coatings [13]. Chang Jiu et al., studied HVOF sprayed TiO_2 coating for photocatalytic applications and reported that fuel flow rate and spray powder had significant influence on phase structure of the coating [14]. Maramossadat et al investigated the HVOF process parameters on properties of nanostructure TiO_2 coating and reported that lower fuel to oxygen ratio preferred for higher percentage of anatase for photo catalytic applications [15].Forghani et al used 2^4 full factorial design to investigate various spraying parameters of TiO_2 coating by

Corresponding author. Tel./fax: +91-9443449869
E-mail address: rsmoorthy32@gmail.com

Atmospheric plasma spray on four important properties of coating microhardness, thickness/cycle, deposition efficiency and porosity [16]. Jaworski et al utilized the 2^3 full factorial design to study the effect of operational spray parameters on mechanical properties such as microhardness and critical load of suspension plasma sprayed TiO_2 coating [17]. Recently, Sheng Hong et al used Taguchi method to optimize the process parameters of HVOF and found the important sequence of spray parameters on hardness of nano structured WC-10Co-4 Cr coating.

However, very little information is available from the open literature regarding the influence of HVOF process parameters on microstructural, mechanical behavior of TiO_2 coating. In this study an attempt has been made to develop empirical relationship to estimate porosity and hardness of TiO_2 coating.

Experimental

Identifying the important process parameters

The initial step in the design of experiments is a choice of variables being process parameters. It has been widely recognized in the thermal spray community that there are many hundred parameters, which can potentially influence the properties of coating. It is time consuming and cost expensive to control all parameters. From the literature [18-19] and trial experiments conducted in our laboratory, the predominant factors which are having more influence on spraying process were identified.
The typical HVOF spray parameters are as follows:

I. Oxygen flow rate (lpm)
II. Fuel flow rate (lpm)
III. Spray distance (mm)
IV. Powder feed rate (gpm)

Identifying working limits of the process parameters

A large number of spraying trials were conducted on grit blasted 2 mm thick Titanium substrate coupons to determine the feasible working limit of HVOF process parameters by varying one parameter and keeping others constant. The chemical composition of the Titanium substrate is shown in Table 1, the chemical composition of Titanium was found by inductively coupled Plasma-Optical Emission Spectroscopy (ICP-OES). During the trial following observations were made.

(i) Oxygen flow rate is less than 252 lpm, the poor adhesion of coating and less flattening of the particles on coating microstructure was observed (Fig 1a). If the oxygen flow rate exceeds the 268 lpm fragmentation of particles and small solidified particles present in coating (Fig 1b).
(ii) If the fuel flow rate is less than 62 lpm lot of unmelted particles was observed in the coating microstructure (fig 1c). For the fuel flow rate 70 lpm more heat was produced, pores, voids present due to splashing of particles and overheating of substrate was observed (fig 1d).
(iii) If the powder feed rate is 28 gpm, very thin coating was formed due to poor deposition of particles (fig 1e). For the powder feed rate of 48 gpm more unmelted particles remain in the coating (fig 1e).
(iv) If the spray distance is less than 216 mm over heating of substrate and more unmelted particles deposited (fig 1g) whereas the distance is more than 240 mm poor deposition was observed (fig 1h).

Trial experiments are carefully conducted and observed the presence of pores, unmelted particles and coating thickness. From the observation the minimum and maximum limits of process parameters were selected which is presented in table 3.

Table 1: Chemical composition of commercially pure Titanium (wt %)

Al	Sn	Fe	Cr	V	Ti
0.0035	0.0195	0.04425	0.00287	0.03737	Remaining

Table 2: Observations during trial

Parameter	Level	Micrograph	observation
Oxygen flow	<252 lpm	1a	poor adhesion of coating coating delamination
	>268 lpm	1b	Fragmentation and small solidified splats
LPG Flow	<62 lpm	1c	More unmelted particles along with melted region
	>70 lpm	1d	Pores , voids and splashing of particles observed
Powder feed rate	<28 gpm	1e	Poor deposition of particles
	>48 gpm	1f	More unmelted particles
Spray distance	<216 mm	1g	Dense and thick unmelted particles
	>216 mm	1h	Poor deposition due to loss of sprayed particles

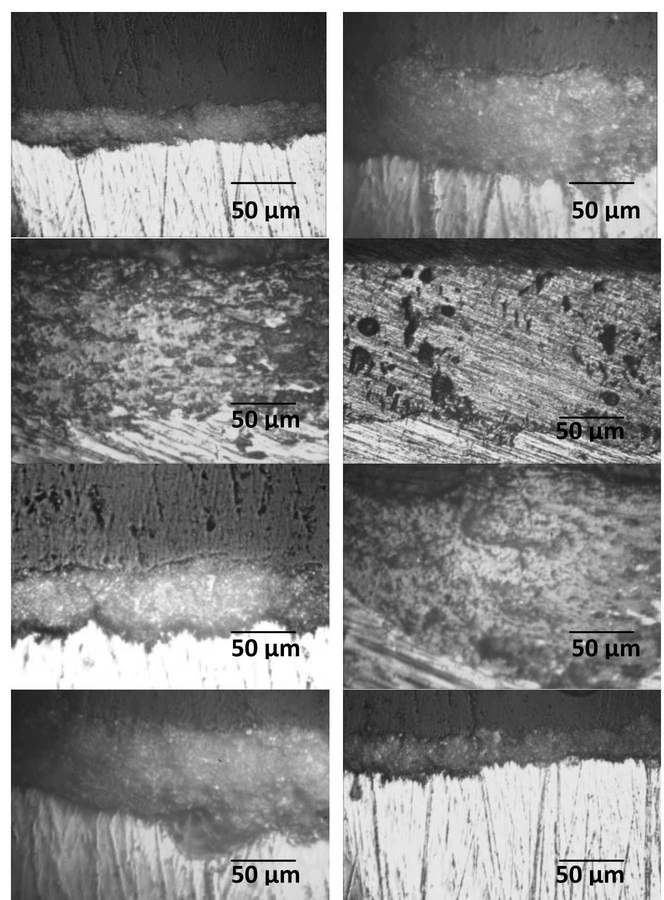

Figure 1: Microstructural observations during HVOF sprayed Titania coating trials

Table 3: The ranges of HVOF spray parameters

No	Factor	Units	Levels				
			-2	-1	0	1	2
1	Oxygen Flow Rate(O)	lpm	252	256	260	264	268
2	LPG Flow Rate (F)	lpm	62	66	70	74	78
3	Powder Feed Rate (P)	g/min	28	33	38	43	48
4	Spray Distance (D)	mm	216	222	228	234	240

Developing the experimental matrix

By considering above conditions, the feasible limits of the parameters were chosen in such a way very good adherent HVOF spray coating was obtained. As the range of individual factor is wide, central composite rotatable four factor five level design matrix has been selected. Central composite rotatable design of second order was found to be the most efficient tool in response surface methodology (RSM) to establish the empirical relationship of the response surfaces using the smallest possible number of experiments without loss of accuracy [20]. Table -3 shows the 30 sets of coded conditions used to form design matrix. First 16 experimental conditions are derived from the design matrix. All the variables at the intermediate (0) level constitute the centre points while the combinations of each process variable at either the lowest (-2) or highest (+2) value with the other four variables of the intermediate levels constitute the star points. Thus 30 experimental conditions allowed the estimation of the linear, quadratic and two-way interactive effects of the variables on porosity and microhardness of HVOF sprayed coating. The method of designing such matrix is dealt elsewhere [21,22]. For the convenience of recording and processing experimental data, the upper and lower levels of the factors have been coded as (-2) and (+2), respectively. The coded values of intermediate values can be calculated using the following relationship:

$$X_i = 2[\,2X - (X_{max} + X_{min})]/[X_{max} - X_{min}] \qquad \text{Eqn} \qquad (1)$$

where X_i is the required coded value of a variable X and X is any value of the variable from X_{min} to X_{max}.

Conducting experiments and recording responses

Powder and HVOF spray process

Fused and crushed Titania (TiO_2) powder feed stock used in this study with size range of 10-45 µm (shown in fig.2). The 25x25x2 mm size Titanium specimens are cut from the as received condition(Optical micrograph is shown in fig.3) and grit blasted by using corundum grits of size 500±320 µm and subsequently cleaned by using acetone in an ultrasonic bath and dried. After grit blasting average surface roughness was measured as 5 µm using surface roughness tester (Make: Mitutoyo, Japan; model Surf test 301). In this study 30 coatings were prepared using different combinations of HVOF spraying parameters as prescribed by the experimental design matrix (Table 4). The experiments were conducted in random order to prevent systematic errors from infiltrating the system. HVOF spraying was carried out using equipment supplied by M/S Metallizing Equipment Co. Pvt. Ltd., Jodhpur, India, which utilizes the supersonic jet generated by the combustion of liquid petroleum gas (LPG) and oxygen mixture. LPG fuel gas is cheap and readily available as compared to other fuels used for HVOF spraying.

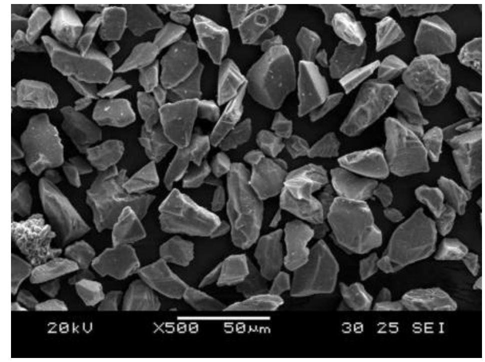

Figure 2: Scanning Electron Micrograph (SEM) of TiO_2 feed stock

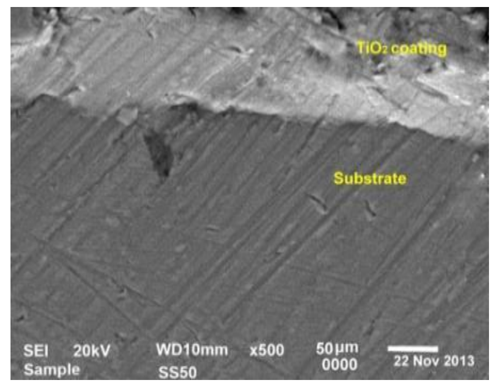

Figure 3: SEM image of TiO_2 coating cross section

Table 4: Design matrix and experimental results

Run	Coded value				Exact values				Response	
	Oxygen flow rate(lpm)	LPG flow rate(lpm)	Powder feed rate(gpm)	Spray distance (mm)	Oxygen flow rate (lpm)	LPG flow rate(lpm)	Powder feed rate (gpm)	Spray distance (mm)	Porosity (vol %)	Hardness ($HV_{0.1}$)
1	-1	-1	-1	-1	256	66	33	222	4	750
2	1	-1	-1	-1	264	66	28	222	2.65	845
3	-1	1	-1	-1	256	74	33	222	2.69	825
4	1	1	-1	-1	264	74	33	222	2.32	898
5	-1	-1	1	-1	256	66	43	222	4.72	739
6	1	-1	1	-1	264	66	43	222	2.62	829
7	-1	1	1	-1	256	74	43	222	2.37	880
8	1	1	1	-1	264	74	43	222	2.6	917
9	-1	-1	-1	1	256	66	33	234	4.37	779
10	1	-1	-1	1	264	66	33	234	1.86	867
11	-1	1	-1	1	256	74	33	234	4	776
12	*1*	*1*	*-1*	*1*	*264*	*74*	*33*	*234*	*3*	*840*
13	-1	-1	1	1	256	66	43	234	5	658
14	1	-1	1	1	264	66	43	234	4.5	740
15	-1	1	1	1	256	74	43	234	4.6	730
16	1	1	1	1	264	74	43	234	3.87	778
17	-2	0	0	0	252	70	38	228	4.56	721
18	2	0	0	0	268	70	38	228	2.8	859
19	0	-2	0	0	260	62	38	228	4.57	712
20	0	2	0	0	260	78	38	228	2.94	824
21	0	0	-2	0	260	70	28	228	2.53	871
22	0	0	2	0	260	70	48	228	4.59	792
23	0	0	0	-2	260	70	38	216	2.94	874
24	0	0	0	2	260	70	38	240	4.54	746
25	0	0	0	0	260	70	38	228	2.17	891
26	0	0	0	0	260	70	38	228	2.24	896
27	0	0	0	0	260	70	38	228	2.17	887
28	0	0	0	0	260	70	38	228	2.8	893
29	0	0	0	0	260	70	38	228	2.06	886
30	0	0	0	0	260	70	38	228	2.14	898

Porosity and Hardness measurement

Metallographic cross section of the coatings was prepared for the porosity and hardness measurements. The samples were carefully cut by diamond cutting machine at slow speed. Then they were mounted with low viscosity epoxy resin under vacuum environment and polished with diamond paste. The porosity of the coatings was carried out on polished cross section as per ASTM B 276 standard [23] using image analysis software equipped with optical microscope (Make : MEIJI, Japan; Model : MIL-7100).

The microhardness measurements was made using Vickers's microhardness tester (Make: Shimnadzu, Japan: Model: HMV – 2T) at 300 g load and 15 s dwell time was used to measure the hardness. The microhardness values were measured at ten random locations on the polished cross section of coating. The Vickers indentation impressions of TiO_2 coatings observed on coating cross sections are shown in fig 4.

Table 5: Experimental conditions of Vickers indentation

Experiment No.	**Parameter**	**Vickers's indentation ($HV_{0.3}$)**	**Observations**
Run 2	O_2 flow rate = 264 lpm Fuel flow = 66 lpm Powder feed = 33 gpm Spray distance = 222 mm	**Figure 4a**	Cracks propagation at the tip of indentation on all directions
Run 8	O_2 flow rate = 264 lpm Fuel flow = 74 lpm Powder feed = 43 gpm Spray distance = 222 mm	**Figure 4b**	No crack initiation and propagation
Run 24	O_2 flow rate = 260 lpm Fuel flow = 70 lpm Powder feed = 38 gpm Spray distance = 240 mm	**Figure 4c**	Severe crack almost all directions

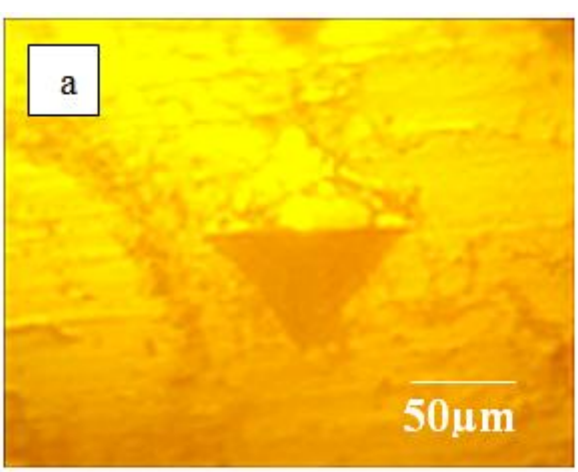

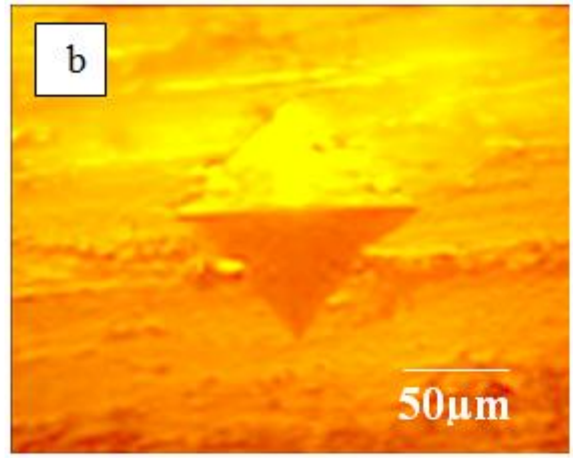

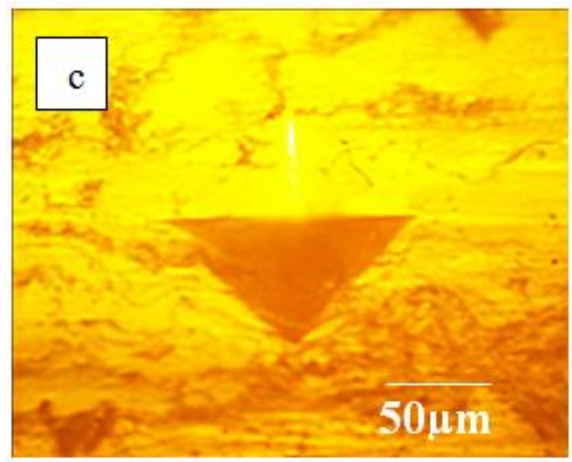

Figure 4: Microhardness indentation images

Development of predictive model for TiO_2 coating

In present study, response surface method was used to predict the response porosity and microhardness of HVOF sprayed coating. Response surface methodology (RSM) is a combination of statistical and mathematical techniques based on a few experiments, which is useful for developing, improving and optimizing HVOF process [24]. To predict the results of experiments with different combinations, second order quadratic model was developed. The responses are function of Oxygen flow rate (O), fuel flow rate (F), Powder feed rate (P), Spray distance (D) and it can be expressed as

$$\text{Responses} = f\,(O, F, P, D) \qquad \text{Eqn (2)}$$

The general form of a quadratic model in several parameters is [25,26] :

$$Y = b_o + \sum b_i x_i + \sum b_{ii}\, x_2 + \sum b_{ij}\, x_i\, x_j \qquad \text{Eqn (3)}$$

For the four factors, the selected polynomial equation can be expressed as

$$Y = b_o + b_1\,(O) + b_2(F) + b_3(P) + b_4(D) + b_{11}(O^2) + b_{22}\,(F^2) + b_{33}(P^2) + b_{44}(D^2) + b_{12}(OF) + b_{13}(OP) + b_{14}(OD) + b_{23}\,(FP) + b_{24}(FD) + b_{34}(PD) \qquad \text{Eqn (4)}$$

Where b_o is a average of responses and b_1, b_2, b_3,........b_{44} are regression coefficients that depend on respective linear, interaction, and square terms of factors. The value of coefficient was calculated using Design Experiment software. After determining the coefficients (at 95% confidence level), the final empirical relationship was developed using these coefficients. The final statistical model to estimate the responses are below:

$$\text{Porosity} = 2.2-0.4O-0.31F+0.39\,P+0.43O\,D+0.28OF+0.13\,C\,O-0.07\,DF-0.15\,FP+0.23\,D\,P+0.25\,D+0.31\,O^2+0.33\,F^2+0.28\,P^2+0.32\,D^2\ \text{vol\%} \quad \text{Eqn (5)}$$

$$\text{Hardness} = 891.8+35.5O+27.5F-19.4\,P-32.1\,D-8.3\,OF-3.9\,OP-0.81\,OD+15\,FP-17.3\,FD-25.2\,PD-24.9O^2-30.4\,F^2+14.5\,P^2-19.9\,D^2\ \text{HV} \quad \text{Eqn (6)}$$

Checking adequacy of the developed model

Analysis of Variance (ANOVA) technique was used to check the adequacy of the developed empirical relationship. In this investigation the desired level of confidence was considered to be 95%. The relationship may be considered to be adequate provided that (a) the calculated value of the 'F' ratio of the model developed should not exceed the standard tabulated value of 'F' ratio and (b) the calculated value of the 'R' ratio of the developed relationship should exceed the standard tabulated value of 'R' ratio for a desired level of confidence. It is found that the model is adequate. The value of probability > F in Table 6 and 7, implied that model is significant. Lack of fit was not significant for all the developed empirical relationship as desired. Fisher's F test with a very low probability value (p model> F= 0.0001) demonstrates a very high significance. The goodness of fit of the model was checked by the determination coefficient (R^2). The coefficient of determination R^2 value was greater than 0.99 indicates that less than 1% of the total variations are not explained by the empirical relationship. The value of adjusted determination coefficient also high indicates the high significance of empirical relationships. Adequate precision compares the range of the predicted values at the design point with the average prediction error. At the same time relatively low value of coefficient of variance indicates the improved precision and the reliability of the conducted experiments [25]. The actual value is compared with predicted value as shown in fig. 5, which indicates that high correlation exist between estimated values and predicted values[26-27].

Table 6: ANOVA for the response Porosity

Source	Sum of Squares	df	Mean Square	F Value	p-value Prob > F	
Model	28.22995	14	2.016425	13.22665	< 0.0001	significant
O	5.850938	1	5.850938	38.37897	< 0.0001	
F	2.362538	1	2.362538	15.49696	0.0013	
P	3.768338	1	3.768338	24.71824	0.0002	
D	4.532704	1	4.532704	29.73207	< 0.0001	
OF	1.316756	1	1.316756	8.637205	0.0102	
OP	0.283556	1	0.283556	1.859975	0.1927	
OD	0.082656	1	0.082656	0.54218	0.4729	
FP	0.400056	1	0.400056	2.624151	0.1261	
FD	0.878906	1	0.878906	5.765147	0.0298	
PD	1.045506	1	1.045506	6.857952	0.0194	
O^2	2.7198	1	2.7198	17.84041	0.0007	
F^2	3.053336	1	3.053336	20.02822	0.0004	
P^2	2.226257	1	2.226257	14.60304	0.0017	
D^2	2.985086	1	2.985086	19.58054	0.0005	
Residual	2.286775	15	0.152452			
Lack of Fit	1.924242	10	0.192424	2.653882	0.1465	not significant
Pure Error	0.362533	5	0.072507			
Cor Total	30.51672	29				
Std. Dev.	0.390451		R-Squared	0.925065		
Mean	3.274		Adj R-Squared	0.855125		
C.V. %	11.9258		Pred R-Squared	0.619694		
			Adeq Precision	12.04316		

CV: coefficient of variance, F: Fisher Ratio; p: probability, df: degree of freedom

Table 7: ANOVA for the response Hardness

Source	Sum of Squares	df	Mean Square	F Value	Prob > F	
Model	145414.6	14	10386.75	339.8683	< 0.0001	significant
A-A	30317.04	1	30317.04	992.0137	< 0.0001	
B-B	18205.04	1	18205.04	595.6931	< 0.0001	
C-C	9087.042	1	9087.042	297.34	< 0.0001	
D-D	24768.38	1	24768.38	810.454	< 0.0001	
AB	1105.563	1	1105.563	36.17547	< 0.0001	
AC	248.0625	1	248.0625	8.116933	0.0122	
AD	10.5625	1	10.5625	0.345619	0.5654	
BC	3630.063	1	3630.063	118.7804	< 0.0001	
BD	4795.563	1	4795.563	156.9172	< 0.0001	
CD	10150.56	1	10150.56	332.1398	< 0.0001	
A^2	17014.53	1	17014.53	556.7378	< 0.0001	
B^2	25358.81	1	25358.81	829.7739	< 0.0001	
C^2	5791.741	1	5791.741	189.5134	< 0.0001	
D^2	10868.81	1	10868.81	355.6419	< 0.0001	
Residual	458.4167	15	30.56111			
Lack of Fit	343.5833	10	34.35833	1.496009	0.3436	Not significant
Pure Error	114.8333	5	22.96667			
Corrected Total	145873	29				
Std deviation	5.52821					
Mean	820.0333					
CV %	0.674145					
R-Squared	0.996857					
Adj R-Squared	0.993924					
Pred R-Squared	0.9853					
Adeq Precision	67.29069					

CV: coefficient of variance, F: Fisher Ratio; p: probability, df: degree of freedom

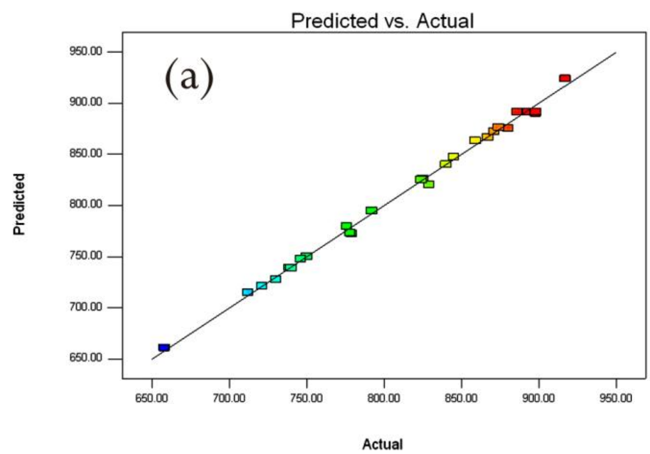

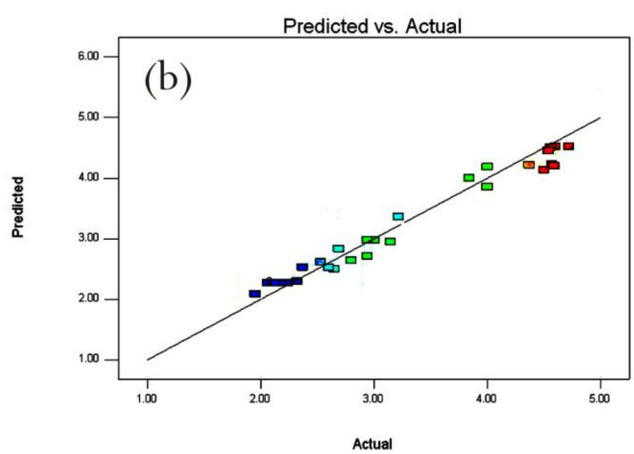

Figure 5: Predicted Vs Actual graph

Results and Discussion

Perturbation plots

Interaction effects of the HVOF process parameters on coating porosity and microhardness were computed and plotted in the form of perturbation graph as shown in fig 6.The perturbation plot is an important diagrammatic representation, which provides silhouette views of the response surface [28]. This graph shows the response changes as each factor moves from chosen reference point, with all other factors held constant at reference value. A steep slope or curvature in a factor indicates that the response is sensitive to the factor. Relatively flat line shows insensitivity to change in that particular factor [29].

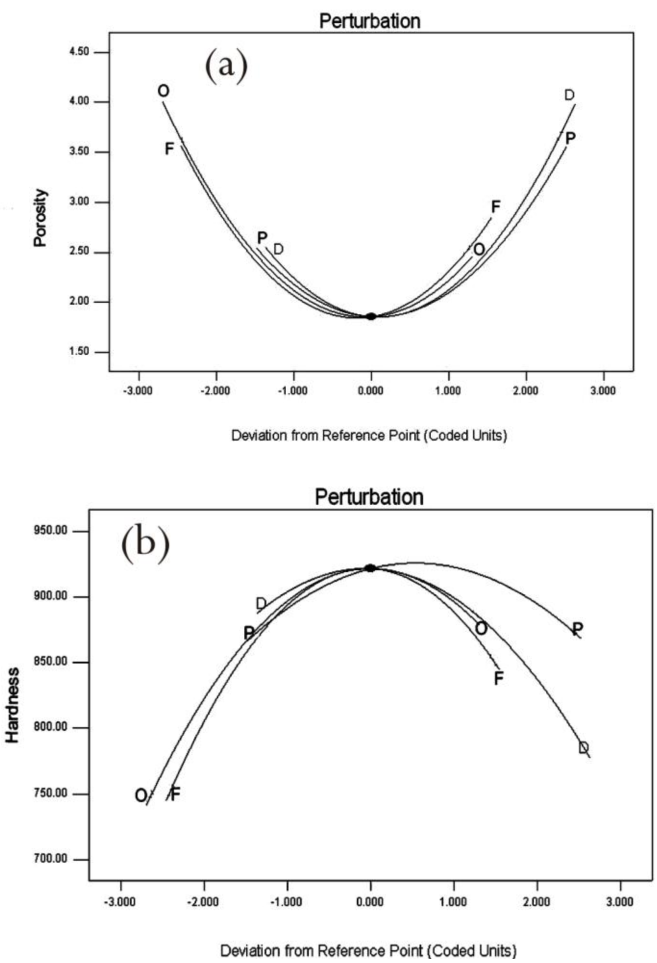

Figure 6: Perturbation Graphs

Porosity and Hardness

From the Analysis of Variance (ANOVA), using F-values, the predominant factor influencing the porosity and hardness of TiO_2 coating is fuel flow rate and spray distance. The perturbation plot (fig-6) shows, porosity decreases with increasing the process parameters, further increase, and the porosity level increases. From the perturbation graph we could understand that at lower fuel flow rate gave improper melting of particles, which resulted in low hardness and high porosity. At low fuel flow, temperature of the flame is insufficient, this is not favours the melting of TiO_2 (melting temperature of the Titania is 1855° C) feed stock and particle or droplet deformation at impact of substrate which leads to incomplete filling causes increase of pore and gives low hardness value.

It can be understood that HVOF process was operated under given oxygen pressure and flow, the flame temperature will be increased with the increase in fuel gas flow under present condition. As a result, the melting condition of spray powder was improved with the increase of fuel gas flow [30-31]. As the more fuel flow rate, increases the flame temperature and velocity of particles. High particle temperature will reduce the viscosity of the droplets, whereas, higher particle velocities will enhance the inter splat contact and reduce coating porosity and increases microhardness [32]. Under very high fuel flow rate, flame temperature and velocity increases drastically. This situation increases the melting of Titania particles and gas entrapment upon impact occurs because of the high pressure in the gas layer just prior to impact. During the rapid spreading and quenching of splats, gas escape can be suppressed resulting in escalating gas pressure in the splat centre, which can create the thin cap of a gas bubble, leaving behind a residual hole causing an increase in porosity level and the reduction of hardness values [33].

From the graph it can be inferred that oxygen flow rate is important parameter influences the flame temperature and velocity. During HVOF spraying process, the powder particles are heated and accelerated at high speed by the combustible gases. The flame temperature reaches maximum value when oxygen content is enough to produce complete combustion of LPG. For higher oxygen flow rate, there is excess oxygen that act as cooling gas and consequently promotes flame temperature decrease [34]. The increasing oxygen flow rate increases the flame velocity and also particle velocity, reducing the residence time of the particle into the flame and consequently reducing the particle temperature. In case of lower oxygen flow rate the there is an excess LPG that act as cooling gas and consequently decreases flame temperature [35]. However the low or high oxygen flow produces more unmelted particles due to cooling of effect happened in the flame, this unmelted particles do not adhere in to the substrate or previously deposited layer that is formed by an unmelted particle, the particle rebound may occur and consequently increases porosity level and decreases hardness [35].

The effect of powder feed rate (curve F) on responses are shown in fig 6. Varying powder feed rate affects the number of particles having to share the kinetic and thermal energies of flame, which in turn affects the particle velocity and temperature. When the powder feed rate is extremely low, most of the particles are melted resulting in quench crack that will increase porosity level and decrease hardness [36]. On other hand, the right quantity of powder feed rate, the molten degree of spray particles which will increase the hardness and decrease the porosity [37].

The variations of responses with spray distances (curve D) are shown in fig 6. It is shown that hardness increases with spray distance reaches maximum and then reduces. A higher spraying distance results in smaller particle velocity towards the substrate producing coating with lower density. Also, by lowering the average impact temperatures of droplets with substrate surface, an increased volume fraction of unmelted particles is produced. Both these effects contribute to a substantial increase in coating porosity [38]. It has been reported that, increasing spray distance the particles were continuously accelerated by a supersonic jet and retarding force worked on particles from entrainment atmosphere. So that the enthalpy of molten ceramic particles is largely lost and particles are decelerated. Under such conditions, the particle striking on substrate will not be flattened to overlap the layers, resulting in higher porosity and reduced hardness value [38, 39]. Lowering spray distance firstly increases deposition rate but problems appear by strongly increasing heat load. Coatings are dense but quenching cracks may form this may promotes porosity thereby reducing hardness [39]. In case of optimum spraying distance, gas jet transfers sufficient temperature and velocity to the particles. The optimum temperature provides more effective packing of splats and better cohesion between splats, hence the decrease in porosity and high hardness was achieved [40].

Relationship between porosity and hardness

The dependence of hardness with porosity can be related by fitting the experimental data in straight line (fig 7). The straight line is governed by the following equation:

$$\text{Microhardness (HV)} = 1035-65.60 \text{ (Porosity)} \qquad \text{Eqn (7)}$$

The slope of the estimated regression equation (- 65.60) is negative, implying that as porosity decreases, microhardness increases. The coefficient of determination is R^2 = 90 %, which can be interpreted as the percentage of the total sum square that can be explained by using the estimated regression equation. The coefficient of determination R^2 is a measure of the goodness of fit of the estimated regression equation [41]. The fitted regression equation line equation (Eq 7) may be used to estimate the mean value of microhardness for the given value of coating porosity and predicting an individual value of coating hardness for a given value of coating porosity level. The confidential interval (CI) and prediction interval (PI) show the precision of regression results. Confidential interval is an interval estimate of the mean value of y for the given value of x. Prediction interval is an interval estimate of an individual value of y for a given value of x. For a given value of coating porosity the estimated regression equation provides a point estimate of mean microhardness value. The difference between CI and PI reflects the fact that it is possible to estimate the mean value of microhardness more precisely than individual. The greater width of the PI reflects the added variability introduced by predicting a value of the random variable as opposed to estimating a mean value. From fig 7, it is inferred that the closer the value to x (2.58%) the narrower the interval.

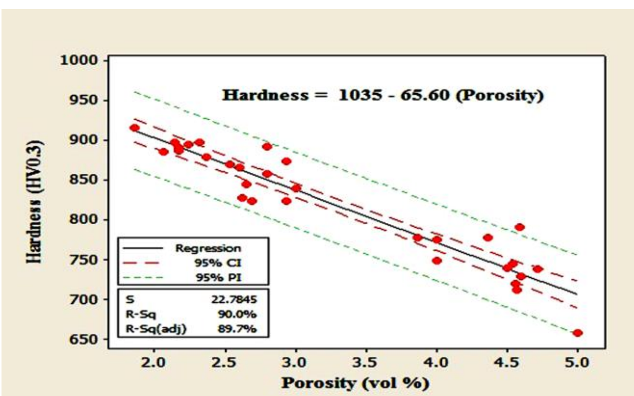

Figure 7: Relationship between porosity and hardness

Conclusions

1. Empirical relationships were developed to predict (at 95% confidence interval) the porosity and microhardness of Titania coatings incorporating predominant spray parameters such as fuel flow, oxygen flow, powder feed rate and spray distance.
2. Among the four HVOF process parameters studied in this investigation, fuel flow has the largest effect on the coating characteristics followed by spray distance, oxygen flow rate and powder feed rate.
3. A linear regression equation was developed between porosity and microhardness of HVOF sprayed TiO_2 coating. The developed relationships can be effectively used to predict the coating porosity and microhardness of the TiO_2 coating.

Acknowledgement

The authors wish to express sincere thanks to Dr. R.Karthikeyan, Associate professor, Arunai College of Engineering and Dr.S.Rajakumar, Assistant Professor, Department of mechanical Engineering, Annamalai University, Chidambaram for their technical support provided to carry out this investigation.

References

1. Y. Paz, A. Heller, Photo-oxidatively self-cleaning transparent titanium dioxide films on soda lime glass: the deleterious effect of sodium contamination and its prevention; Journal of Materials Research: 12, 1997, 2759.
2. Jean-Marie Herrmann, Heterogeneous photocatalysis: fundamentals and applications to the removal of various types of aqueous pollutants; Catalysis Today: 53 (1), 1999, 115.
3. M. Miki-Yoshida, V. Collins-Martinez, P. Amezaga-Madrid, A.Aguilar-Elguezabal, Thin films of photocatalytic TiO2 and ZnO deposited inside a tubing by spray pyrolysis; Thin Solid Films: vol. 419.1, 2002, pp. 60-64.
4. Thermal Spray Materials Guide, Sulzer Metco Inc., issued February 2006, AP-51, PDF file, July 30, 2007.
5. G.E. Kim, J. Walker Jr., J.B. Williams Jr., 2004, Nanostructured Titania coated titanium; US Patent 6,835,449 B2: December 28, 2006.
6. B.R. Marple, M.M. Hyland, Y.C. Lau, R.S. Lima, J. Voyer ; Proven and promising applications of thermal sprayed nanostructured coatings; Building on 100 Years of Success: Proceedings of the International Thermal Spray Conference: Seattle, WA,USA, May 2006, 15–18.
7. P. Fauchais, in: S.J. Schneider Jr. (Ed.), Engineered Materials Handbook, Ceramic and Glasses, vol. 4, ASM International, Materials Park, OH, USA, 1991, p. 202.
8. M. Miyayama, K. Koumoto, H. Yanagida, in: S.J. Schneider Jr. (Ed.), Engineered Materials Handbook, Ceramic and Glasses, vol. 4, ASM International, Materials Park, OH, USA, 1991, p. 748.
9. A. Ibrahim, R.S.Lima, C.C.Bernt, B.R.Marple, Fatigue and mechanical properties of nanostructured and conventional titania (TiO_2) thermal spray coatings; Surface & Coatings Technology: 201, 2007, pp- 7589–7596.
10. D.Thirumalaikumarasamy, K.Shanmugam, V.Balasubramanian, Influences of atmospheric plasma spraying parameters on the porosity level of alumina coating on AZ31B magnesium alloy using response surface methodology; Progress in Natural Science: Materials International: 22(5), 2012, 468–479.
11. E. Dongmo, M Wenzelburger, R Gadow, Analysis and optimization of the HVOF process by combined experimental and numerical approaches; Surface & Coatings Technology: vol.202.18, 2008, pp. 4470–4478.
12. L.Gil, Influence of HVOF parameters on the corrosion resistance of NiWCrBSi Coatings; Thin Solid Films: 420 –421,2002, pp. 446–454.
13. Chang-Jiu Li, Phase Formation during Deposition of TiO_2 Coatings through High Velocity Oxy-Fuel Spraying; Materials Transactions: Vol. 47, No. 7, 2006, pp. 1690 to 1696.
14. Maryamossadat, Bozorgtabar, Mehdi salehi, Mohammadreza Rahimipour, Mohammadreza Jaffarpour, Influence of High velocity oxy-fuel parameters on properties of nanostructured TiO_2 coatings; Bull, Material science: vol 33, December 2010, page 671-675.
15. S.M. Forghani, M.J.Ghazali,A.Muchtar, A.R.Daud, N.H.N.Yusoff, C.H.Azhari, Effects of plasma spray parameters on TiO_2-coated mild steel using design of experiment(DoE) approach; Ceramics International: Vol.39, 2013, pp. 3121–3127.
16. R.Jaworski et al, Characterization of mechanical properties of suspension plasma sprayed TiO_2 coating using scratch test, surface coating technology 202(2008) 2644-2653.
17. Gaona, M, Influence of particle temperature and velocity on the microstructure and mechanical behaviour of high velocity oxy-fuel (HVOF)-sprayed nanostructured titania coatings, Journal of Materials Processing Technology, 198, 1-3, pp. 426-435, 2008
18. Kim, George E., Jimmy Walker Jr, and John B. Williams Jr, Nanostructured titania coated titanium; U.S. Patent No. 6,835,449. 28 Dec. 2004..
19. S.Rajakumar, C.Muralidharan, V.Balasubramanian, Establishing empirical relationships to predict grain size and tensile strength of friction stir welded AA 6061-T6 aluminium alloy joints; Transaction Non Ferrous Materials Society: Vol.20, 2010, pp.1863–72.
20. R.G. Miller, J.E. Freund, D.E. Johnson, Probability and Statistics for Engineers, Prentice Hall of India Pvt. Ltd, New Delhi, 1999.

21. D.C. Montgomery, Design and Analysis of Experiments, John Wiley & Sons Ltd, New Delhi, 2007.
22. ASTM B276-05, Standard Testing Method for Apparent Porosity in Cemented Carbides; vol. 02.05., American Society for Testing and Materials, Pennsylvania, 2010.
23. Myers RH, Montgomery DC. Response surface methodology: process and product optimization using designed experiments. New York: John Wiley and Sons; 2002.
24. A.S. Shahi and S. Pandey, Modelling of the Effects of Welding Conditions on Dilution of Stainless Steel Claddings Produced by Gas Metal Arc Welding Procedures, Journal of Materials Processing Technology: vol 196, 2008, pp. 339-344.
25. Box GEP, Hunter WH, Hunter JS, Statistics for experiments, New York: John Wiley Publications; 1978.
26. Miller JE, Freund, Johnson R. Probability and statistics for engineers, vol.5. New Delhi: Prentice Hall; 1996.
27. G.E.P. Box and N.R. Draper, Empirical Model-Building and Response Surfaces, John Wiley & Sons, Inc., New York, 1986
28. V.Balasubramanian, A.K.Lakshminarayanan, R.Varahamoorthy and S.Babu, Understanding the parameters controlling plasma transferred arc hard facing using response surface methodology, Materials Manufacturing process, 23(2008) 674-682.
29. Li, Mingheng, and Panagiotis D. Christofides, Modeling and Control of High-Velocity Oxygen-Fuel (HVOF) Thermal Spray: A Tutorial Review; Journal of thermal spray technology: vol.18.5-6, 2009, pp. 753-768.
30. M.P. Planche, B.Normand, H.Liao, G.Rannou, C.Coddet, Influence of HVOF spraying parameters on in-flight characteristics of Inconel 718 particles and correlation with the electrochemical behaviour of the coating; Surface and coatings technology: vol.157.2, 2002, pp. 247-256.
31. M. Gaona, Influence of particle temperature and velocity on the microstructure and mechanical behaviour of high velocity oxy-fuel (HVOF)-sprayed nanostructured Titania coatings; Journal of materials processing technology: vol.198, 2008, pp. 426–435.
32. G. Montavon, C.C. Berndt, C. Coddet, S. Sampath, and H.Herman, Quality Control of the Intrinsic Deposition Efficiency from the Controls of the Splat Morphologies and the Deposit Microstructure; Journal of Thermal Spray Technology:Vol.6, 1997, pp.153-166.
33. W. Rush, Thermal Spray 2007: Global Coatings Solutions; Beijing, China, ASM International, May14–16 2007, pp. 572.
34. Josep A. Picas, Influence of HVOF spraying parameters on the corrosion resistance of WC–Co-Cr coatings in strong acidic environment; Surface & Coatings Technology: vol.225, 2013, pp. 47–57.
35. Lopes, M.A., Monteiro, F.J., Santos, J.D., Glass-reinforced composites: fracture toughness and hardness dependence on microstructural characteristics; Biomaterials: vol. 20,1999, pp. 2085–2090.
36. S. Kuroda, T. Fukushima, and S. Kitahara, Significance of Quenching Stress in the Cohesion and Adhesion of Thermally Sprayed Coatings; Journal of Thermal Spray Technology: vol.1, 1992, pp 325-332.
37. Qun Wang, The parameters optimization and abrasion wear mechanism of liquid fuel HVOF sprayed bimodal WC–12Co coating, Surface & Coatings Technology 206 (2012) 2233–2241.
38. L.Gil, Influence of HVOF parameters on the corrosion resistance of NiWCrBSi Coatings, Thin Solid Films 420 –421 (2002) 446–454.
39. C.S. Ramachandran, V. Balasubramanian, and P.V. Ananthapadmanabhan, Multiobjective Optimization of Atmospheric Plasma Spray Process Parameters to Deposit Yttria-Stabilized Zirconia Coatings Using Response Surface Methodology; Journal of Thermal Spray Technology: Vol.20, 2010, pp.590-607.
40. S.Rajakumar, C.Muralidharan, V.Balasubramanian, Developing empirical relationships to predict grain size and hardness of the weld nugget of friction stir welded AA7075-T6 aluminium alloy joints; Experimental Techniques: vol.36, 2012, pp. 6–17.